Infrared Multiple Photon Dissociation of Chloromethyltrifluorosilane

Pavel V. Koshlyakov*[1], Sergey R. Gorelik[1,2,3], Evgeniy N. Chesnokov[1,2], Oleg S. Aseev[1,2], Asylkhan A. Rakhymzhan[1,2] and Alexander K. Petrov[1]

[1]Institute of Chemical Kinetics and Combustion SB RAS, Institutskaia, 3, Novosibirsk, Russia
[2]Novosibirsk State University, Pirogova, 2, Novosibirsk, Russia
[3]Institute of Material of Research and Engineering, 3, Research Link, Singapore

ABSTRACT

Infrared multiphoton absorption and dissociation of chloromethyltrifluorosilane molecules under the action of pulsed transversely excited atmospheric pressure CO_2 laser were experimentally studied. Dissociation products were analyzed. The dissociation proceeds *via* chlorine atom transfer from carbon to silicone. High degrees of silicon isotope separation were achieved. The presence of α-chlorine atom in a silicon organic compound brings about a significant improvement in multiple photon dissociation characteristics and an essential increase in isotopic selectivity.

INTRODUCTION

In the past decade, interest in the applications of isotopically pure silicon materials for semiconductor technology has been growing worldwide, in particular, after the thermal conductivity of highly enriched ^{28}Si had been found to be almost 60% higher than that of naturally abundant Si at room temperature (1). Subsequently, this result was redefined (2): It was found that the enhancement of thermal conductivity was about 10% at room temperature, whereas at low temperatures the thermal conductivity of isotopically pure Si exceeds that of naturally abundant Si by a factor of 8.

In the opinion of experts (3), the outlook for technological applications of ^{28}Si is quite optimistic. However, one of the main obstacles for using isotopically pure ^{28}Si on the technological scale is the cost of its production by means of traditional isotope separation methods. This requires an effective isotope separation process for Si. Laser isotope separation involving infrared multiphoton dissociation (IR MPD) is one of the most promising ways to satisfy the demand because of the high selectivity of this method (4,5).

This makes it relevant to study the MPD of silicon-containing molecules in order to find the most appropriate compounds for the laser-induced silicon isotope separation technology.

Silicon has three stable isotopes with the natural composition 92.22% (^{28}Si): 4.69% (^{29}Si): 3.09% (^{30}Si) (6). Separation of Si isotopes by means of the infrared laser radiation has been studied (7–14). The most impressive results were achieved in experiments on MPD of the species Si_2F_6 (9–13). Kamioka *et al.*

(9,10) reported that the MPD of Si_2F_6 molecules induced by CO_2 laser radiation had significantly high dissociation efficiency and high isotope selectivity under mild radiation fluences lower than 1 J cm^{-2}. The enrichment coefficient (selectivity) reached 30 for the ^{30}Si isotope and 6 for the ^{29}Si isotope.

Despite the impressive results, it is not evident that Si_2F_6 might be considered as the best object for silicon isotope separation by means of IR MPD. The molecule contains two Si atoms and the rare isotopes are contained mostly in "isotopically mixed" molecules such as ^{28}SiF$_3$-$^{29(30)}$SiF$_3$. This fact limits the isotopic effect as during the dissociation of these "isotopically mixed" molecules, the ^{28}Si isotope and the rare one (^{29}Si or ^{30}Si) would pass into products equally. In addition, we could expect that the isotopic shift in the molecular vibrational frequencies in the "isotopically mixed" molecules should be less than that in the isotopically "pure" molecules.

Silicon isotope-selective MPD of compounds containing single silicon atoms, such as SiH_2F_2 (15), $SiF_3C_6H_5$ (16–18), SiF_3CH_3 (19,20), SiF_3CHCH_2 (21) and $Si(OCH_3)_4$ (22) was studied previously. The maximum isotope selectivities reached for the MPD of these molecules were found to be lower than that for Si_2F_6. From the analysis of spectroscopic and kinetic characteristics of the MPD of these molecules, one can conclude that the main reason for the higher efficiency of the Si_2F_6 MPD is its low dissociation threshold (188 kJ mol^{-1} [10]) compared to the molecules studied elsewhere (around 420 kJ mol^{-1} [14–22]). Therefore, the further search of the compounds should be limited to those containing only one silicon atom, and possessing a relatively low dissociation threshold.

Haszeldine *et al.* (23–27) studied experimentally the thermal decomposition of halogenoalkylsilanes. They showed that the halogenoalkylsilane compounds, in which halogen is present at α- or β-carbon relative to silicon, essentially easily underwent the unimolecular decomposition *via* the intramolecular rearrangement involving the unimolecular transfer of halogen from carbon to silicon. It was shown that dissociation with the β-halogen atom transfer proceeds *via* a four-center transition state and leads to the formation of stable products, olefin and halogen-substituted silane:
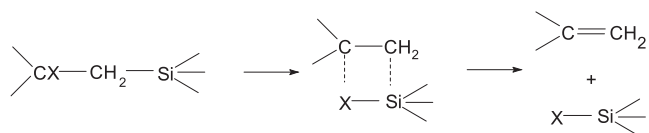
*Corresponding author email: pvk@kinetics.nsc.ru (Pavel V. Koshlyakov)

Similar transfer of α-halogen proceeds *via* a three-center transition state and is followed by the formation of halogen-substituted silane and carbene.

In particular, the kinetics of pyrolysis of fluoroalkylsilanes was studied (23). The decomposition of such molecules with either α- or β-fluorine took place at fairly low temperatures, less than 200°C, while the molecules containing no fluorine atom in α- or β-position were stable under these conditions. Dissociation energies obtained from the kinetics data were within the range of 100–160 kJ mol^{-1} (23).

So low dissociation energies make the unimolecular decay reactions of halogenoalkylsilanes proceeding *via* the halogen atom transfer from carbon to silicon a promising way for the isotope-selective MPD. In this study we report the experimental study of the silicon isotope selective decomposition of SiF_3CH_2Cl molecules induced by pulsed transversely excited atmospheric (TEA) pressure CO_2 laser irradiation. This molecule contains the α-chlorine atom, and the dissociation of this molecule occurs *via* the chlorine atom transfer from carbon to silicon:

$$SiF_3CH_2Cl \rightarrow :CH_2 + SiF_3Cl \qquad (R.1)$$

The dissociation products are methylene and trifluorochlorosilane. The silicon isotope composition of the latter product varies depending on the frequency of the laser radiation.

MATERIALS AND METHODS

Chemicals. SiF_3CH_2Cl was synthesized by the reaction of $SiCl_3CH_2Cl$ with antimony trifluoride and consequently purified using a homemade low-temperature rectification column. Reaction yield was 40%. $SiCl_3CH_2Cl$ was received from the A. E. Favorsky Irkutsk Institute of Chemistry SB RAS.

Radiation source. A homemade tunable pulse TEA CO_2-laser was used as a source of IR radiation. The maximum pulse energy of the laser was about 5 J. The laser beam was collimated in front of the input window of the cell with the aperture 1 cm in diameter. The energy of the laser radiation pulse was varied by changing the discharge energy and pressure in the laser cavity. To change the pulse energy significantly, a set of parallel-sided CaF_2 plates was used. The average energy of the laser radiation was measured in front of the cell and after the cell with an optical powermeter. The unfocused uniform laser beam was used through all the experiments.

Experimental. All the experiments were performed under batch cell conditions at room temperature. Samples of chloromethyltrifluorosilane with natural abundance of silicon isotopes were irradiated. The reaction cell was a Pyrex-glass cylinder with NaCl windows. The cell length was 42 cm; the cell diameter was 3 cm. The cell content was analyzed with a MH-1303 mass spectrometer. The cell was continually connected to the ion source of the mass spectrometer through a glass pinhole about 20 μm in diameter. Therefore, the cell content could be analyzed at any moment during the laser irradiation. The concentration and isotope composition of SiF_3CH_2Cl were determined from the $m/e = 132$–138 lines of the mass spectrum. The concentration and isotope composition of the SiF_3Cl MPD product were determined from the $m/e = 120$–124 lines of the mass spectrum. The isotope analysis of these species was complicated by the superposition of the mass spectra of the compounds containing different chlorine and silicon isotopes. To overcome this problem, a special software was designed to determine the composition of ^{35}Cl-^{37}Cl and ^{28}Si–^{29}Si–^{30}Si isotopes taking into account all the lines in the mass spectrum. The corresponding algorithm is described in the Appendix.

The IR spectra were measured with a Fourier transform infrared (FTIR) spectrometer (Bruker Vector 22) with the spectral resolution of 1 cm^{-1}.

Computational details. Geometry calculations of the reactants, products and intermediates were performed with the GAUSSIAN98 suite of programs (28). Those were fully optimized and the funda-mental frequencies were calculated using the density functional theory at the hybrid B3LYP level (29,30) with the 6-31G(p,d) basis set and the unrestricted formalism for the case of radicals. The geometries of transition states (TS) were found using the QST2 procedure (31) and then optimized. The TS geometries were confirmed by frequency calculations of the same level of theory, presenting one imaginary frequency corresponding to the transition vectors pointing in the direction of the reaction coordinate. The structures of local minima (reactant and products) were also confirmed through frequency calculations. This shows that all the frequencies are necessarily real at local minima.

RESULTS AND DISCUSSION

Infrared spectrum

The FTIR spectrum of chloromethyltrifluorosilane (1 cm^{-1} resolution) containing most of the fundamental vibrational bands of the molecule is shown in Fig. 1. Two strong absorption bands correspond to the stretching vibrational modes of the SiF_3 group of the molecule. The DFT calculations of the fundamental frequencies of the SiF_3CH_2Cl molecule were performed to assign the vibrational bands in the IR spectrum. The molecule has a plane of symmetry. Therefore, all the vibrations are divided into two groups: A′—symmetrical with respect to the plane, and A′—antisymmetrical with respect to the plane. The calculated vibrational frequencies, as well as those obtained from the IR spectrum, are shown in Table 1.

To estimate the isotopic shifts in the IR spectrum, the vibrational frequencies of minor Si isotopomers of the molecule were calculated in this spectral region. The results are shown in the third and fourth columns of Table 1. For the stretching vibrations of the SiF_3 group of chloromethyltrifluorosilane molecules, the calculated isotopic shift for the Si isotopically substituted molecules was found to be about 7–8 cm^{-1} for the molecules containing ^{29}Si and about 15–16 cm^{-1} for the molecules containing ^{30}Si with respect to ^{28}Si-containing molecules. These values are typical for the Si isotopic shifts in the IR spectra of fluorosilanes in the spectral region of Si–F stretching vibrations (32).
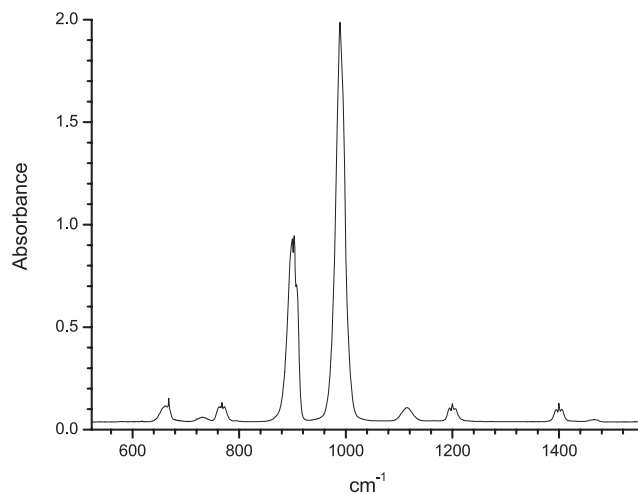

Figure 1. FTIR spectrum of chloromethyltrifluorosilane (1 cm^{-1} resolution), containing the major part of the fundamental vibrational bands of the molecule. Vapor pressure SiF_3CH_2Cl was 3 torr, length of the reaction cell 18 cm.

Table 1. Calculated and experimental values of vibrational frequencies of SiF_3CH_2Cl isotopomers.

| | Calculated (B3LIP) Scaling factor = 0.96 | | | | | |
	^{28}Si	^{29}Si	^{30}Si	Symmetry	Experiment	Type of vibration
1	46.8	46.8	46.8	A″	–	Torsion
2	108.1	108.0	107.9	A′	–	Si–C–Cl bending
3	196.0	195.9	195.8	A″	–	Si–C–Cl rock
4	222.9	222.8	222.7	A′	–	F–Si–C bending
5	304.8	303.8	303.0	A″	–	SiF_3 bending
6	317.7	316.6	315.6	A′	–	SiF_3 bending
7	379.3	377.4	375.6	A′	–	?
8	623.9	622.9	621.9	A′	668	Si–C stretching
9	724.9	724.9	724.9	A″	731	CH_2 rock
10	725.4	725.4	725.4	A′	768	C–Cl stretching
11	863.8	858.0	852.7	A′	903	Si–F stretching
12	968.6	960.2	952.2	A′	989	Si–F stretching
13	977.3	969.2	961.6	A″	989	Si–F stretching
14	1095.9	1095.3	1094.7	A″	1115	CH_2 twist
15	1192.9	1192.5	1192.3	A′	1201	CH_2 wag
16	1399.0	1399.0	1399.0	A′	1400	CH_2 scissors
17	2969.0	2969.0	2969.0	A′	2955	C–H stretching
18	3026.7	3026.7	3026.7	A″	–	C–H stretching

Sample molecules were excited with the CO_2-laser radiation in the region of Si–F stretching vibrational band at 989 cm^{-1}.

Estimation of dissociation threshold for SiF₃CH₂Cl decomposition

As was mentioned above, we expected the reaction (R.1) to be the main channel of SiF_3CH_2Cl decomposition, with SiF_3Cl and CH_2 products. The ground state of methylene, CH_2, is triplet. Due to the spin conservation law, methylene should be formed in the singlet excited state in reaction (R.1). The energy difference between the fundamental triplet state and the first excited singlet state for methylene is about 38 kJ mol^{-1} (33).

The B3LYP calculation of the enthalpy change in reaction (R.1) gives: $\Delta H = 368$ kJ mol^{-1}. The activation energy is a more important characteristic of the decomposition process. However, we could not find the transition state (saddle point at the potential energy surface) between the reactant SiF_3CH_2Cl and the products $SiF_3Cl + {}^1CH_2$ using the QST2 procedure. We calculated the potential surface along one specific trajectory connecting the reactant with the products. For this trajectory, the activation threshold was not higher than the energy of the reaction products. Hence, the activation threshold of the unimolecular decomposition of SiF_3CH_2Cl to $SiF_3Cl + {}^1CH_2$ is equal to the energy change of the reaction, *i.e.* 368 kJ mol^{-1}.

The energy change in the SiF_3CH_2Cl decomposition *via* Si–C bond cleavage, $SiF_3CH_2Cl \rightarrow SiF_3 + CH_2Cl$, was calculated to be 381 kJ mol^{-1}.

Infrared multiphoton absorption and dissociation

Figure 2 presents the laser fluence dependence of $<n>$—the average number of absorbed photons per molecule, measured at 10R (18) CO_2-laser line (977.2 cm^{-1}).

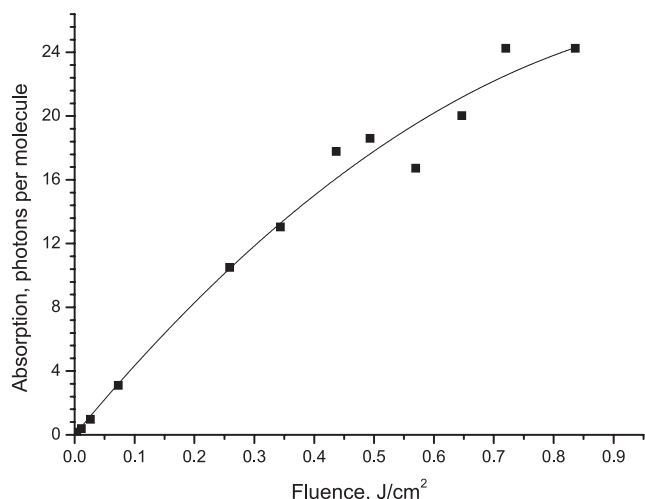When the laser fluence is lower than 0.5 J cm^{-2}, the dependence is linear. The average number of absorbed photons

Figure 2. Laser fluence dependence of $<n>$—the average number of absorbed photons per molecule, measured at 10R (18) CO_2-laser line (977.2 cm^{-1}) at 300 mtorr sample pressure. Solid line: polynomial fitting of experimental points (see text for details).

per molecule reaches 17 at 0.5 J cm^{-1} of the laser fluence. The corresponding absorption cross-section, derived from the slope of the dependence, was found to be 8×10^{-19} cm^2. It is close to the linear cross-section, which could be determined from the IR spectrum in Fig. 1 (8.8×10^{-19} cm^2).

Figure 3 presents the laser fluence dependence of IR MPD probability β, an average probability of a single molecule to dissociate during the single laser pulse, for SiF_3CH_2Cl molecules. It was measured at 10R (18) CO_2-laser line. Sample pressure was 0.1 torr. For comparison, the same data for Si_2F_6 molecules (34), SiF_2H_2 molecules (15) and SiF_3CH_3 (19) are shown.

Dissociation probability β for SiF_3CH_2Cl molecules becomes measurable at fluences higher than 0.2 J cm^{-2} and reaches several percent at the laser fluence of about 0.6 J cm^{-2}. SiF_3CH_2Cl molecules dissociate more effectively than difluorosilane because the latter possess the rotational bottleneck (15). At the same time, SiF_3CH_2Cl molecules dissociate
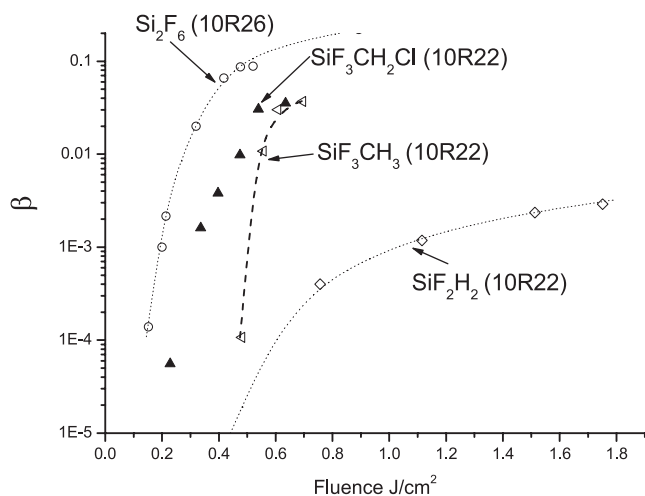

Figure 3. Laser fluence dependence of IR MPD probability for SiF_3CH_2Cl molecules at 10R (18) CO_2-laser line, sample pressure 0.1 torr. Same dependences for Si_2F_6 molecules (29), SiF_2H_2 molecules (12) and SiF_3CH_3 (15) are shown.

less effectively than hexafluorodisilane, apparently because the dissociation energy of the latter is essentially lower—about 188 kJ mol^{-1} (10).

Note that the MPD of SiF$_3$CH$_3$, for which SiF$_3$CH$_2$Cl is the chlorine-substituted derivative, could be observed only at laser fluences higher than 0.4 J cm^{-2}. Thus, the insertion of chlorine atom into the α position was followed by an essential decrease in the multiple photon dissociation threshold.

Reaction products and secondary reactions

The mass spectrometric analysis of the reaction cell contents after irradiation shows that the main products of dissociation are SiF$_3$Cl, C$_2$H$_4$ and C$_2$H$_2$. Other products, such as SiF$_4$, SiF$_3$CH=CH$_2$, SiF$_3$CH$_2$–CH$_2$Cl and HCl, are present in small amounts. The product composition confirms that the dissociation proceeds *via* Cl atom transfer from carbon to silicon:
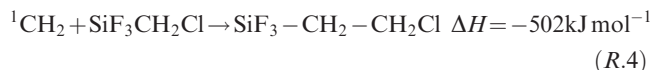
$$\text{SiF}_3\text{CH}_2\text{Cl} + n h\nu \rightarrow \text{SiF}_3\text{Cl} + {}^1\text{CH}_2 \qquad (R.2)$$

The rate constants of the relaxation of singlet methylene in collisions with polyatomic molecules

$$^1\text{CH}_2 + \text{M} \rightarrow {}^3\text{CH}_2 + \text{M} \qquad (R.3)$$
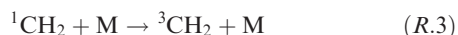
are essentially high $(1–2) \times 10^{-10}$ cm^3 s^{-1} (33,35). ^{1}CH$_2$ reactions with hydrocarbons are very fast, with rate constants approaching the gas kinetic collision efficiency, while the corresponding rate constants of ^{3}CH$_2$ are 5–6 orders of magnitude lower (33).

Therefore, the end products are formed not only in primary dissociation reaction (R.2) but also in secondary reactions of ^{1}CH$_2$ formed in reaction (R.2). In particular, ^{1}CH$_2$ can undergo insertion reactions (35–39). Therefore, the presence of SiF$_3$CH$_2$–CH$_2$Cl in the end products of the dissociation of SiF$_3$CH$_2$Cl in our experiments could be explained by the insertion of ^{1}CH$_2$ into the Si–C bond of SiF$_3$CH$_2$Cl:

$$^1\text{CH}_2 + \text{SiF}_3\text{CH}_2\text{Cl} \rightarrow \text{SiF}_3-\text{CH}_2-\text{CH}_2\text{Cl} \quad \Delta H = -502 \, \text{kJ mol}^{-1}$$
$$(R.4)$$

SiF$_3$–CH$_2$–CH$_2$Cl is formed with an excess of energy, therefore it could dissociate, producing SiF$_3$CH=CH$_2$:

$$\text{SiF}_3\text{C}_2\text{H}_4\text{Cl} \rightarrow \text{SiF}_3\text{C}_2\text{H}_3 + \text{HCl} \quad \Delta H = 82 \, \text{kJ mol}^{-1} \quad (R.5)$$

All ΔH values were calculated using the B3LYP method.

Hydrocarbon products resulting from the dissociation of SiF$_3$CH$_2$Cl are formed in reactions:

$$^1\text{CH}_2 + {}^1\text{CH}_2 \rightarrow \text{C}_2\text{H}_2 + \text{H}_2 \qquad (R.6)$$

$$^3\text{CH}_2 \rightarrow (\text{wall}) \rightarrow 1/2 \, \text{C}_2\text{H}_4 \qquad (R.7)$$
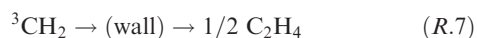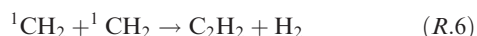
From the above consideration, we can conclude that, qualitatively, the end product composition confirms the primary dissociation channel to be the dissociation of SiF$_3$CH$_2$Cl into SiF$_3$Cl + ^{1}CH$_2$.

Isotope-selective MPD of SiF$_3$CH$_2$Cl

Figure 4 shows the dependence of the reaction yield on the laser radiation wavenumber–MPD spectrum (squares). It

was experimentally obtained by tuning the CO$_2$ laser through the laser lines. Sample pressure was 0.1 torr, the laser fluence was kept constant about 0.3 J cm^{-2}. Under these conditions, the dissociation probability did not exceed 0.2%.

The width of the MPD spectrum shown in Fig. 4 is about 12–15 cm^{-1}. As shown above, the isotope shifts in the frequency of ^{29,30}Si–F stretching vibrations with respect to ^{28}Si–F are about 8 cm^{-1} for ^{29}Si and 16 cm^{-1} for ^{30}Si correspondingly. Thus, the width of the MPD spectrum is comparable with the isotope shifts, or even lower. Therefore we can expect the isotopic selectivity of SiF$_3$CH$_2$Cl multiphoton dissociation to be relatively high. However, the frequencies of the silicon isotope-substituted molecules are close to the gap between the R and P branches of the CO$_2$-laser, where the laser does not emit. This gas is indicated in Fig. 4 by two solid vertical lines. This gap could make it impossible to achieve the optimal conditions for a highly selective Si isotope MPD of SiF$_3$CH$_2$Cl molecules in our experiments.

Figure 5 presents typical dependence of relative concentrations of different silicon isotopes on irradiation time for the sample molecule (a) and for the SiF$_3$Cl product (b) in our experiments. The time when the laser was turned on is indicated with a dashed vertical line. Before that, the laser was turned off. A decrease in the concentration during this period is caused by gas consumption in the mass-spectrometer. The laser was tuned to the 10P (19) laser line, the repetition rate was 0.5 Hz. Concentrations of molecules with different Cl isotopes were summed up.

Assuming the first-order reaction, the following expressions for the concentrations of different isotopomers of reagent SiF$_3$C$_2$H$_3$Cl$_2$ and product SiF$_3$Cl can be obtained:

$$\frac{n^{28}(t)}{n_0^{28}} = \exp\left(-k^{28} \cdot t\right) \quad p^{28}(t) = n_0^{28} \cdot \left(1 - \exp\left(-k^{28} \cdot t\right)\right) \quad (1)$$

where $n^{28}(t)$ and $p^{28}(t)$ are the concentrations of the reagent and the product molecules containing ^{28}Si, respectively, k^{28} is the effective first-order rate constant and t is irradiation time.
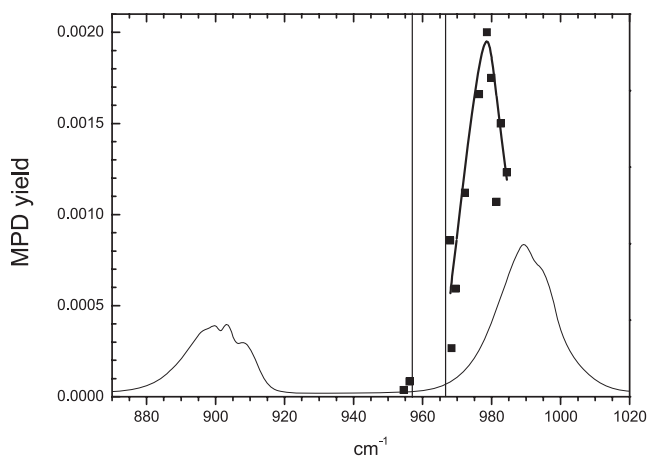

Figure 4. Dependence of the probability of the MPD of SiF$_3$CH$_2$Cl molecules on the laser radiation wavenumber–MPD spectrum (squares). Sample pressure was 0.1 torr, the laser fluence was about 0.3 J cm^{-2}.
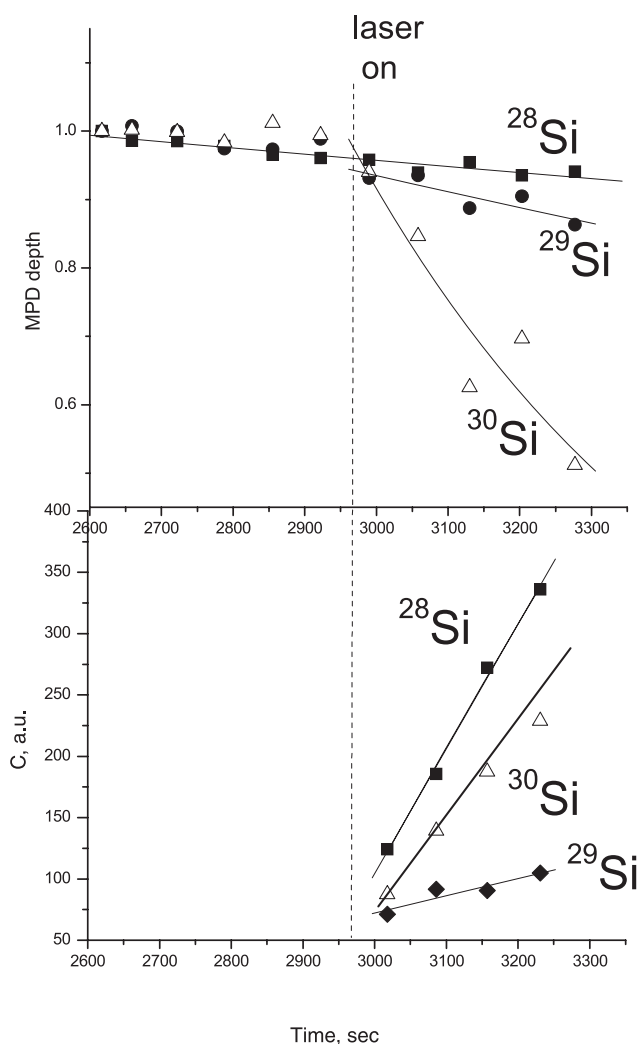
Figure 5. Typical dependences of relative concentrations of different silicon isotopes on irradiation time in the sample molecule (a) and in the SiF$_3$Cl product (b) in our experiments.

Similar expressions could be written for the concentrations of the molecules containing ^{29}Si and ^{30}Si.

The initial region of product concentration growth could be approximated by linear function

$$p^{28}(t) = n_0^{28} \cdot k^{28} \cdot t; \ p^{29}(t) = n_0^{29} \cdot k^{29} \cdot t; \ p^{30}(t) = n_0^{30} \cdot k^{30} \cdot t \tag{2}$$

The ratio of the first-order rate constants can be used as a measure of the isotopic selectivity:

$$S_{30} = \frac{k^{30}}{k^{28}} \quad S_{29} = \frac{k^{29}}{k^{28}} \tag{3}$$

The effective rate constants can be determined either from the decay of the reagent concentration or from the growth of the product concentration. For ^{28}Si and ^{29}Si, the decay of the reagent concentration is considerably affected by gas consumption in the mass spectrometer. Therefore, the rate constants can be determined more accurately from the growth of the products. Using the linear approximation (Eq. 2) we obtain:

$$S_{30} = \frac{k^{30}}{k^{28}} = \frac{n_0^{28}}{n_0^{30}} \cdot \frac{w_{30}}{w_{28}} \quad S_{29} = \frac{k^{29}}{k^{28}} = \frac{n_0^{28}}{n_0^{29}} \cdot \frac{w_{29}}{w_{28}} \tag{4}$$

where $w_{28} = \mathrm{d}p^{30}/\mathrm{d}t$ is the rate of ^{30}SiF$_3$Cl formation, w_{28} is the rate of ^{28}SiF$_3$Cl formation and w_{30} is the rate of ^{30}SiF$_3$Cl formation.

From the initial region of growing product concentration (Fig. 5b): $w_{30}/w_{28} = 0.8$.

Taking into account the fact that the silicon isotope composition of the sample molecules before the irradiation was equal to the natural one: $\eta_{28} = 92.2\%$—the abundance of ^{28}Si and $\eta_{30} = 3.1\%$—the abundance of ^{30}Si, we obtain for selectivity S:

$$S_{30} = \eta_{28} \cdot w_{30}/(\eta_{30} \cdot w_{28}) = 24 \tag{5}$$

One can see from Fig. 5b that the rate of the growth of the ^{30}SiF$_3$Cl product decreases during irradiation. Consistent with Eq. (1), this decrease is due to the fast consumption of the sample molecules with ^{30}Si. According to the isotope composition analysis of the sample molecules, nearly a half of ^{30}SiF$_3$CH$_2$Cl dissociated during the first 260 s of irradiation, whereas the concentration of ^{28}SiF$_3$CH$_2$Cl changed insignificantly during the same time. Therefore, the concentration of the ^{28}SiF$_3$Cl molecules continues to increase at the same rate.

Figure 6 presents the spectral dependences of the selectivities for ^{30}Si and ^{29}Si determined using Eq. (5). The dependences were obtained by tuning the laser through different laser lines in the P- and R-branches. The initial pressure of SiF$_3$CH$_2$Cl was 0.1 torr. The laser fluence was within the range 0.27–0.3 J cm^{-2}. When the laser radiation was tuned into the R-branch, the enrichment of products with ^{28}Si isotope was observed. In the P-branch of laser radiation, the products were enriched with ^{30}Si, ^{29}Si isotopes. The spectral range 955–970 cm^{-1} was not available for measurements, as it corresponds to the gap between R- and P-branches of the laser radiation. The maximal selectivity achieved in our experiments was $S_{30} = 44$. This value is comparable with the values achieved by Kamioka *et al.* in experiments with Si$_2$F$_6$ (9,10).

CONCLUSION

The presence of α-chlorine atom in organosilicon compounds brings about a significant improvement in multiple photon
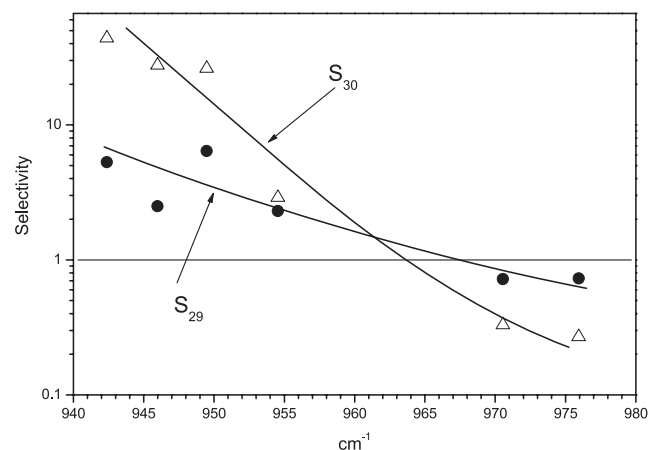

Figure 6. Spectral dependences of the selectivities for ^{30}Si and ^{29}Si.

dissociation characteristics, which causes an essential increase in isotopic selectivity.

However, the studied molecule is not an optimal choice for the technological applications from the following point of view: a singlet methylene biradical is formed as a primary product of the dissociation. It is involved in the complex secondary reactions, including the reaction with the parent molecules. The latter reaction is isotopically nonselective, therefore it limits the selectivity. A desirable choice would be the molecule which dissociates into molecular products only. The silicon organic molecules with β-chlorine or fluorine atoms should dissociate to molecular products. One could expect that the study of such molecules will allow one to achieve more efficient multiphoton dissociation and higher silicon isotope selectivities.

APPENDIX

Isotope analysis of SiF$_3$Cl and SiF$_3$CH$_2$Cl compounds

The mass spectrum of SiF$_3$Cl contains a group of lines with $m/e = (120–124)$, which corresponds to different chlorine and silicon isotope variations of the parent ion SiF$_3$Cl$^+$. Let us denote the intensities of these lines as $H_{120},\dots,H_{124}$, and their relative intensities as

$$h_i = \frac{H_i}{\sum\limits_{j=120}^{124} H_j}$$

Relative intensities could be derived using different contents of chlorine and silicon isotopes:

$$h_{120} = (1-x)(1-y-z) \qquad (A1)$$

$$h_{121} = (1-x)y \qquad (A2)$$

$$h_{122} = (1-x)z + x(1-y-z) \qquad (A3)$$

$$h_{123} = xy \qquad (A4)$$

$$h_{124} = xz \qquad (A5)$$

Here x is ^{37}Cl content, y is ^{29}Si, z is ^{30}Si content.

Hence, we have to determine the set of variables x, y and z so that the intensities $h_{120} \dots h_{124}$ fit the experimental mass spectrum in the best way. Applying the chi-square method, we have to find a minimum of the function of three variables:

$$S(x,y,z) = [h_{120} - (1-x)(1-y-z)]^2 + [h_{121} - (1-x)y]^2$$
$$+ [h_{122} - (1-x)z - x(1-y-z)]^2$$
$$+ (h_{123} - xy)^2 + (h_{124} - xz)^2$$
$$(A6)$$

MS Excel "search of solution" function was used to find numerically the minimum of $S(x,y,z)$. As a result, Cl, Si isotope composition in SiF$_3$Cl was obtained. The chlorine isotope composition $x = 0.231 \pm 0.005$ was slightly different from the natural one, 0.2447 (4). Silicon isotope composition varied in a wide range depending on the laser irradiation wavelength. The algorithm <became> nonrobustness appeared when the samples highly enriched with ^{30}Si were analyzed. In these cases, the solution looked like the samples were highly enriched with the ^{37}Cl isotope. To overcome this, the chlorine isotope composition was frozen at $x = 0.231$. Only the silicon isotope composition was varied.

The isotope analysis of SiF$_3$CH$_2$Cl was performed using the group of mass spectrum lines $m/e = (132–138)$. Not only the parent ion SiF$_3$CH$_2$Cl$^+$ contributes to these lines but also fragment ions SiF$_3$CHCl$^+$ and SiF$_3$CCl$^+$, which complicates the isotope analysis. Denoting the relative contribution of the SiF$_3$CHCl$^+$ ion as p and that of SiF$_3$CCl$^+$ as q, we obtain for the relative line intensities $h_{132}\dots h_{138}$:

$$h_{132} = q(1-x)(1-y-z) \qquad (A7)$$

$$h_{133} = p(1-x)(1-y-z) + q(1-x)y \qquad (A8)$$

$$h_{134} = (1-p-q)(1-x)(1-y-z) + p(1-x)y + q((1-x)z$$
$$+ x(1-y-z)) \qquad (A9)$$

$$h_{135} = (1-p-q)(1-x)y + p((1-x)z + x(1-y-z)) + qxy \qquad (A10)$$

$$h_{136} = (1-p-q)((1-x)z + x(1-y-z)) + pxy + qxz \qquad (A11)$$

$$h_{137} = (1-p-q)xy + pxz \qquad (A12)$$

$$h_{138} = (1-p-q)xz \qquad (A13)$$

Using the chi-square method, we need to find the minimum of the function of five variables. Its expression is similar to (A6), and is not shown here due to its complexity.

The analysis of SiF$_3$CH$_2$Cl before irradiation allowed for determination of its isotope composition and relative probabilities of the fragment ion formation: $P = 0.015$ и $q = 0.006$. In subsequent analysis, these two variables were assumed to be the same. Therefore, the problem of determining the isotope composition of SiF$_3$CH$_2$Cl using the group of mass lines $m/e = (132–138)$ was reduced to the search of the minimum of the function of three variables.

Table A1. Mass spectra of SiF$_3$Cl and SiF$_3$CH$_2$Cl. Each mass spectrum was normalized to its most intensive line.

m/e	SiF$_3$Cl	SiF$_3$CH$_2$Cl	m/e	SiF$_3$Cl	SiF$_3$CH$_2$Cl
			85	100	28.9
26	6.46	0.21	86	4.3	1.50
27	1.61	0.48	87	2.03	0.95
28	3.68	2.42	98	0.15	1.58
31	0.08	1.09	99	0.55	70.3
32		0.78	100	1.19	4.99
33	0.60	50.7	101	38.6	5.23
34		0.51	102	3.09	0.23
35	3.87	2.27	103	11.8	0.74
47	7.00	26.4	104	1.15	0.15
48	0.40	5.87	114		2.03
49	0.48	34.8	115		15.5
50	0.12	1.88	116		1.64
51	0.22	10.6	117		5.30
52	0.69	0.14	120	74.1	0.10
61	0.73	0.11	121	3.38	0.03
62	1.37	0.09	122	25.7	0.03
63	1.26	0.28	123	1.08	
66	2.90	4.90	124	0.54	
67	0.17	6.20	132		1.30
69		1.54	133		2.98
79	0.18	0.63	134		100
80	0.15	1.12	135		7.08
81	0.13	0.97	136		35.5
82	1.15	0.28	137		2.02
83	1.73	0.27	138		1.08

REFERENCES

1. Ruf, T., R. W. Henn, M. Asen-Palmer, E. Gmelin, M. Cardona, H. J. Pohl, G. G. Devyatych and P. G. Sennikov (2000) Thermal conductivity of isotopically enriched silicon. *Sol. St. Commun.* **115**, 243.
2. Kremer, R. K., K. Graf, M. Cardona, G. G. Devyatykh, A. V. Gusev, A. M. Gibin, A. V. Inyushkin, A. N. Taldenkov and H.-J. Pohl (2000) Thermal conductivity of isotopically enriched ^{28}Si: Revisited. *Sol. St. Commun.* **131**, 499.
3. Business Wire. FindArticles.com (2004) Isotopically Pure Silicon-28 Recognized by International Semiconductor Industry. Available at: http://findarticles.com/p/articles/mi_m0EIN/is_2004_March_9/ai_114045413. Accessed on 9 March 2004.
4. Bagratashvili, V. N., V. S. Letokhov, A. A. Makarov and E. A. Ryabov (1985) *Multiple Photon Infared Laser Photophysics and Photochemistry*. Harwood Academic Publ., New York.
5. Letokhov, V. S. (1989) *Laser Spectroscopy of Highly Vibrationally Excited Molecules*. Adam-Hilger, Bristol.
6. Lide, D. R. (ed.) (1998) *CRC Handbook of Chemistry and Physics*, 79th edn, CRC Press, Boca Raton, FL.
7. Lyman, J. L. and S. D. Rockwood (1976) Enrichment of boron, carbon, and silicon isotopes by multiple-photon absorption of 10.6 μm laser radiation. *J. Appl. Phys.* **47**, 595–601.
8. Serdyuk, N. K., E. N. Chesnokov and V. N. Panfilov (1981) Vibrational excitation effects on silane reactivity in its reaction with bromine atoms. *React. Kinet. Catal. Lett.* **17**, 19.
9. Kamioka, M., S. Arai, Y. Ishikawa, S. Isomura and N. Takamiya (1985) ^{29}Si and ^{30}Si enrichment by IR MPD of Si$_2$F$_6$. *Chem. Phys. Lett.* **119**, 357–360.
10. Kamioka, M., Y. Ishikawa, H. Kaetsu, S. Isomura and S. Arai (1986) Isotope-selective infrared multiple photon decomposition of hexafluorodisilane. *J. Phys. Chem.* **90**, 5727–5730.
11. Suzuki, H., H. Araki and T. Noda (1997) Enrichment of silicon isotopes by infrared laser irradiation. *J. Jpn. Inst. Met.* **61**, 145.
12. Lyman, J. L., B. E. Newman, T. Noda and H. Suzuki (1999) Enrichment of silicon isotopes with infrared free-electron laser radiation. *J. Phys. Chem. A* **103**, 4227–4232.
13. Arai, S., H. Kaetsu and S. Isomura (1991) Practical separation of silicon isotopes by IRMPD of Si$_2$F$_6$. *Appl. Phys. B* **53**, 199–202.
14. Polianski, M., O. V. Boyarkin, T. R. Rizzo, V. M. Apatin, V. B. Laptev and E. A. Ryabov (2003) Infrared laser chemistry of trichlorosilane in view of silicon isotope separation. *J. Phys. Chem. A* **107**, 8578–8583.
15. Gorelik, S. R., E. N. Chesnokov, L. V. Kuibida, R. R. Akberdin and A. K. Petrov (2004) Infrared multiphoton dissociation of difluorosilane. *Appl. Phys. B* **78**, 119–125.
16. Petrov, A. K., A. V. Chernyshev, E. N. Chesnokov, S. R. Gorelik, L. V. Kuibida, K. Nomaru and H. Kuroda (2002) Separation of silicon isotopes in IR multiphonon dissociation of trifluorophenylsilane induced by a free-electron laser. *Doklady Akademii Nauk* **385**(5), 638. [In Russian]
17. Chernyshev, A. V., K. Nomaru, A. K. Petrov, E. N. Chesnokov, S. R. Gorelik, L. V. Kuibida, R. R. Akberdin and H. Kuroda (2003) Isotope selective dissociation of phenyltrifluorosilane under free electron laser irradiation. *J. Phys. Chem. A* **107**(44), 9362–9367.
18. Baranov, V. Y., A. P. Dyad'kin and V. A. Kuz'menko (1990) Isotopically selective dissociation of CH$_3$SiF$_3$ and C$_6$H$_5$SiF$_3$ molecules by CO$_2$ laser pulses. *J. Quantum Electron.* **20**, 450. [In Russian]
19. Koshlyakov, P. V., E. N. Chesnokov, S. R. Gorelik and A. K. Petrov (2006) Infrared multiphoton dissociation of methyltrifluorosilane. *Russ. J. Phys. Chem. B* **25**(5), 22.
20. Alimpiev, S. S., A. M. Velichko, S. M. Nikiforov, G. L. Odobashyan, B. G. Sartakov and S. V. Sin'ko (1988) Time-of-flight photo-ionization of products of infrared dissociation of silicon containing molecules. *Pis'ma v Zhurnal Tekhnicheskoi Fiziki* **14**, 1786. [In Russian]
21. Koshliakov, P. V., S. R. Gorelik, E. N. Chesnokov, A. V. Vorobiev and A. K. Petrov (2006) Infrared multiphoton dissociation of vinyltrifluorosilane. *Appl. Phys. B* **84**, 529.
22. Laptev, V. B., L. M. Tumanova and E. A. Ryabov (1998) Selective dissociation of Si(OCH$_3$)$_4$ and [(CH$_3$)$_3$Si]$_2$O molecules under action of pulsed CO2 laser radiation. *High Energy Chem.* **32**, 108. [In Russian]
23. Fishwick, G., R. N. Haszeldine, C. Parkinson, P. J. Robinson and R. F. Simmons (1965) Kinetics of the thermal decomposition of polyfluoroalkylsilicon compounds. *J. Chem. Soc, Chem. Common.*, 382.
24. Bevan, W. I., R. N. Haszeldine, J. Middleton and A. E. Tipping (1970) Novel thermal rearrangements involving interchange between groups on silicon and those on its α-carbon. *J. Organomet. Chem.* **23**, 17.
25. Haszeldine, R. N., P. J. Robinson and R. F. Simmons (1967) The kinetics of the reactions of silicon compounds. Part II. The gas-phase thermal decomposition of 3,3,3-trifluoropropyltrifluorosilane. *J. Chem. Soc. B*, 1357.
26. Haszeldine, R. N., P. J. Robinson and R. F. Simmons (1964) The kinetics of the reaction of silicon compounds. Part I. The gas-phase thermal decomposition of 2,2-difluoroethyltrifluorosilane. *J. Chem. Soc. B*, 1890.
27. Graham, D., R. N. Haszeldine and P. J. Robinson (1971) Kinetics of the reactions of silicon compounds. Part VII. Unimolecular gas-phase thermal decomposition of 2,2-difluoroethyltrimethoxysilane. *J. Chem. Soc. B*, 611.
28. Frisch, M. J., G. W. Trucks, H. B. Schlegel, G. E. Scuseria, M. A. Robb, J. R. Cheeseman, V. G. Zakrzewski, J. A. Montgomery Jr, R. E. Stratmann, J. C. Burant, S. Dapprich, J. M. Millam, A. D. Daniels, K. N. Kudin, M. C. Strain, O. Farkas, J. Tomasi, V. Barone, M. Cossi, R. Cammi, B. Mennucci, C. Pomelli, C. Adamo, S. Clifford, J. Ochterski, G. A. Petersson, P. Y. Ayala, Q. Cui, K. Morokuma, D. K. Malick, A. D. Rabuck, K. Raghavachari, J. B. Foresman, J. Cioslowski, J. V. Ortiz, A. G. Baboul, B. B. Stefanov, G. Liu, A. Liashenko, P. Piskorz, I. Komaromi, R. Gomperts, R. L. Martin, D. J. Fox, T. Keith, M. A. Al-Laham, C. Y. Peng, A. Nanayakkara, C. Gonzalez, M. Challacombe, P. M. W. Gill, B. G. Johnson, W. Chen, M. W. Wong, J. L. Andres, M. Head-Gordon, E. S. Replogle and J. A. Pople (1998) Revision A.6–A.11. Gaussian, Inc., Pittsburgh, PA.
29. Becke, A. D. (1993) Density-functional thermochemistry. III. The role of exact exchange. *J. Chem. Phys.* **98**, 5648.
30. Lee, C., W. Yang and R. G. Parr (1988) Development of the Colle-Salvetti correlation-energy formula into a functional of the electron density. *Phys. Rev. B* **37**, 785.

31. Curtiss, L. A., K. Raghavachari, G. W. Trucks and J. A. Pople (1991) Gaussian-2 theory for molecular energies of first- and second-row compounds. *J. Chem. Phys.* **94**, 7221.
32. Chesnokov, E. N., P. V. Koshlyakov and S. R. Gorelik (2005) Absorption bands in IR spectrum of methyltrifluorosilane. Calculation and comparison with experiment. *Optika i Spektroskopiya* **99**(6), 923. [In Russian]
33. Hancock, G. and M. R. Heal (1992) Temperature dependences of methylene (~a 1A1) removal rates by argon, nitric oxide, hydrogen, and ketene in the range 295–859 K. *J. Phys. Chem.* **96**, 10316.
34. Okamura, H., V. Tosa, T. Ishii and K. Takeuchi (1996) Collisional effects in the IR multiphoton absorption and dissociation of Si_2F_6. *J. Photochem. Photobiol. A* **95**, 203.
35. Kirmse, W. (1971) *Carbene Chemistry*, 2nd edn. Academic, New York.
36. Roth, J. J. (1971) Photolysis of diazomethane in tetrachloromethane. Abstraction reaction of singlet methylene. *Am. Chem. Soc.* **93**, 1527.
37. March, J. (1986) *Advanced Organic Chemistry*, 3rd edn. Wiley, New York.
38. Krzyzanowski, S. and R. J. Cventanovic (1967) Relative rates of reaction of olefins with the ground and the first excited electronic states of methylene. *Can. J. Chem.* **45**, 665.
39. Bradley, J. N. and A. Ledwith (1963) The reactions of carbenes and diazoalkanes with ketones. Part I. The reaction of carbene with acetone. *J Chem. Soc.*, 3480.